

## Astrometric Measurements of Double Star Systems HEI 915, GRV 719, STI 2170, and RST 2531.

Nathan Bowman<sup>1</sup>, Karthikeya Vattem<sup>1,2</sup>, Sophia Bhatti<sup>1,3</sup>, Kavi Bidlack<sup>1,4</sup>, Kalée Tock<sup>1</sup>

<sup>1</sup> Stanford Online High School, Redwood City, CA; [nathanlbowman@gmail.com](mailto:nathanlbowman@gmail.com)

<sup>2</sup> Independence High School, Frisco, TX

<sup>3</sup> Unionville High School, Kennett Square, PA

<sup>4</sup> Design Tech High School, Redwood City, CA

### Abstract

The double star systems HEI 915, GRV 719, STU 2170, and RST 2531 were measured and analyzed in order to investigate the relationship of their component stars. Images were requested of each system from the Las Cumbres Observatory Global Telescope network and were measured for the position angle and separation. Historical data was also used to plot the position of the secondary star relative to the primary star for each system. Some of the systems appeared to have somewhat of a linear trend, though this was inconclusive. Finally, system escape velocity was calculated for all of the stars. Although all four systems are co-located and co-moving, indicating a physical relationship, all four have relative velocities that exceed the corresponding system escape velocity, suggesting that they are unlikely to be gravitationally bound. GRV 719's relative velocity only slightly exceeded its escape velocity, which may suggest that its stars could be gravitationally bound within the uncertainty in the calculations.

### 1. Introduction

WDS 05319+2220 HEI 915, WDS 06415+3045 GRV 719, WDS 06588+5532 STI 2170, and WDS 08094-3836 RST 2531 are double stars located in the constellations Taurus, Gemini, Lynx, and Puppis respectively. These stars have not been measured for several years, with HEI 915 last measured in 2014 (Zacharias et al., 2015), GRV 719 in 2016 (El-Badry, 2021), STI 2170 in 2015 (Zacharias et al., 2015), and RST 2531 in 1999 (Skrutsie, 2006), so the measurements of this paper offer an update. Furthermore, each system has interesting characteristics. The secondary of HEI 915 was once listed as a variable (Bronnikova, 1975), but it does not currently appear in the AAVSO Variable Star Index (Kloppenborg, 2023). The stars of RST 2531 are part of the “Gaia red clump,” which are red giant stars of similar luminosities that can be used as standard candles (L. Ruiz-Dern et al., 2018). In addition, RST 2531 is a triple system, and the secondary B component of RST 2531 has a potentially binary companion in the system RST 2531 BC.

While variable in their locations and features, these targets were all selected from the Washington Double Star catalog based on similar criteria including their magnitude, separation, and classification as physical doubles. They all have a secondary star magnitude of less than 13 and a delta magnitude of less than 3 to ensure that both stars of the system will be visible and resolved in images with a consistent exposure time on the Las Cumbres Observatory Global Telescope (LCOGT) network instruments used. The separation was constrained to be above 5" so that the stars can be properly measured without overlap in the images,

and below 15" to increase the likelihood of a strong physical relationship. They are also identified on Stelle Doppie as physical doubles.

The Gaia G absolute magnitude, estimated spectral type, and estimated mass for each star was retrieved from the Gaia astrophysical parameters table. For stars where these parameters were not provided, Gaia Data Release 3 (DR3) parallax and apparent magnitude can be used with Eq. (1), along with the Gaia BP-RP color, to plot each star's position on the Gaia HR diagram (Gaia Collaboration, 2023; 2016b; 2023j).

$$M = m + 5 * (\log p + 1) \quad (1)$$

In Equation 1, M is the absolute G-filter magnitude, m is the apparent G-filter magnitude, and p is the parallax. Gaia BP-RP color on the x-axis of the Gaia HR diagram is a proxy for surface temperature, and Gaia G absolute magnitude on the y-axis is a proxy for luminosity. Figure 1 was used to estimate spectral type and temperature based on Gaia BP-RP color and Gaia G absolute magnitude, as shown in Table 1. Figure 2 was then used to estimate mass. However, Figure 2 estimated masses were only used for the primary of GRV 719 and the secondary of RST 2531, and the other star masses were taken from Gaia data. All four systems are on the Main Sequence near the turnoff point. In Table 1, the Gaia G absolute magnitude, Estimated spectral type, and Estimated mass columns were queried from the Gaia DR3 Astrophysical Parameters table as LUM\_FLAME, SPECTRALTYPE\_ESPHS, and MASS\_FLAME, respectively.

Table 1. Spectral type and mass estimates from Gaia. Bold values were not provided by the Gaia data and are calculated or estimated based on Eq. (1), Fig. 1, and Fig. 2.

System	Primary or Secondary	Parallax (mas)	Gaia source ID	Gaia G apparent magnitude	Gaia G absolute magnitude	BP-RP color	Estimated spectral type	Estimated mass
HEI 915	Primary	3.45885 ± 0.0286	34040322 03677401 216	10.55	5.36	0.702	F	1.4
	Secondary	3.56317 ± 0.0178	34040321 99382932 096	11.53	1.66	0.967	F	0.9
GRV 719	Primary	2.6536 ± 0.0215	34350309 02501081 600	11.42	<b>3.54</b>	0.967	G	<b>1.5</b>
	Secondary	2.6303 ± 0.0174	34350309 06797222 400	11.78	2.21	0.838	G	1.1
STI 2170	Primary	2.09331 ± 0.0259	99996439 19150859 52	12.04	2.5	0.811	G	1.0
	Secondary	2.01821 ± 0.0274	99996431 88983334	12.10	2.58	0.822	G	1.1

			40					
RST 2531	Primary	4.7590 ± 0.0149	55409761 73741665 152	9.98	3.40	0.715	F	1.3
	Secondary	5.3248 ± 0.5422	55409761 73729454 336	11.25	<b>4.50</b>	0.945	<b>F</b>	<b>1.5</b>

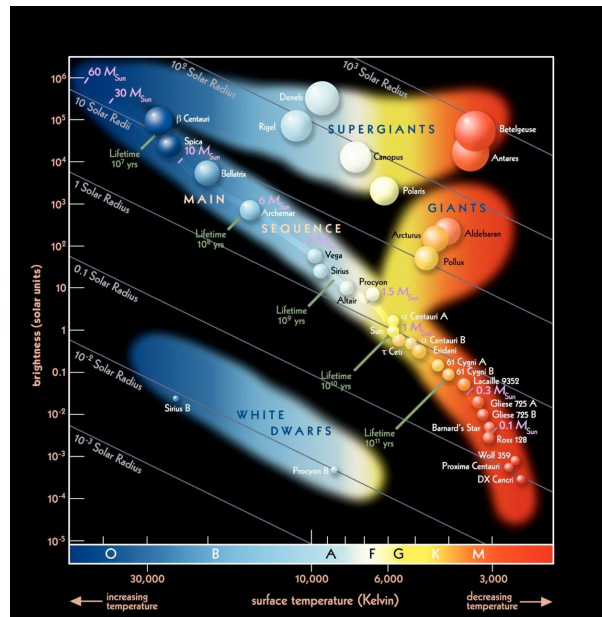
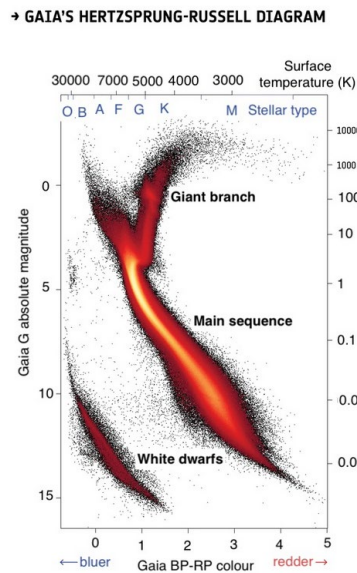


Figure 1 (left): Gaia HR Diagram (Gaia Collaboration et al., 2023; Gaia Collaboration et al., 2016b; Gaia Collaboration et al., 2023j). Figure 2 (right): HR diagram (ESO) with known masses labeled.

## 2. Instruments Used

Images of each system were requested through the online LCOGT network portal (Brown et al., 2013). Images of HEI 915 and GRV 719 were taken from the Teide Observatory in Tenerife, Spain. The images of STI 2170 were taken from the McDonald Observatory in Texas, USA, and the images of RST 2531 were taken from the Siding Spring Observatory in New South Wales, Australia.

All systems were imaged using the PlaneWave DeltaRho 350 + QHY600, which has a field of view of 30' x 30' in central mode, and a format of 2400 x 2400 pixels. Ten images were requested for each system. HEI 915, GRV 719, and RST 2531 were taken using the Bessell-V filter (Bessell, 1990) with exposure times of 9.5 seconds, 22.1 seconds, and 10 seconds respectively. These exposure times were calculated using the online LCOGT Exposure Time Calculator. For the system STI 2170, the V-filter exposure time was

computed to be 46 seconds, so in order to save telescope time, the exposure time was halved and the wider-bandpass PanSTARRS-w filter (Tonry et al., 2012) was used instead.

### 3. Data

The images were analyzed using AstroImageJ. Some images were re-requested because of technical problems with the original returned images, but all images were ultimately well-resolved. Fig. 3 contains screenshots of one sample measurement of each system. The image of HEI 915 shows an elongated primary star that may be related to an associated 20th magnitude star identified by Gaia. RST 2531’s B component features a potentially binary companion that was not resolved in any of the images. Table 2 lists the summary measurements for each system after image reduction, including the size of the measurement aperture used and the decimal date of observation.

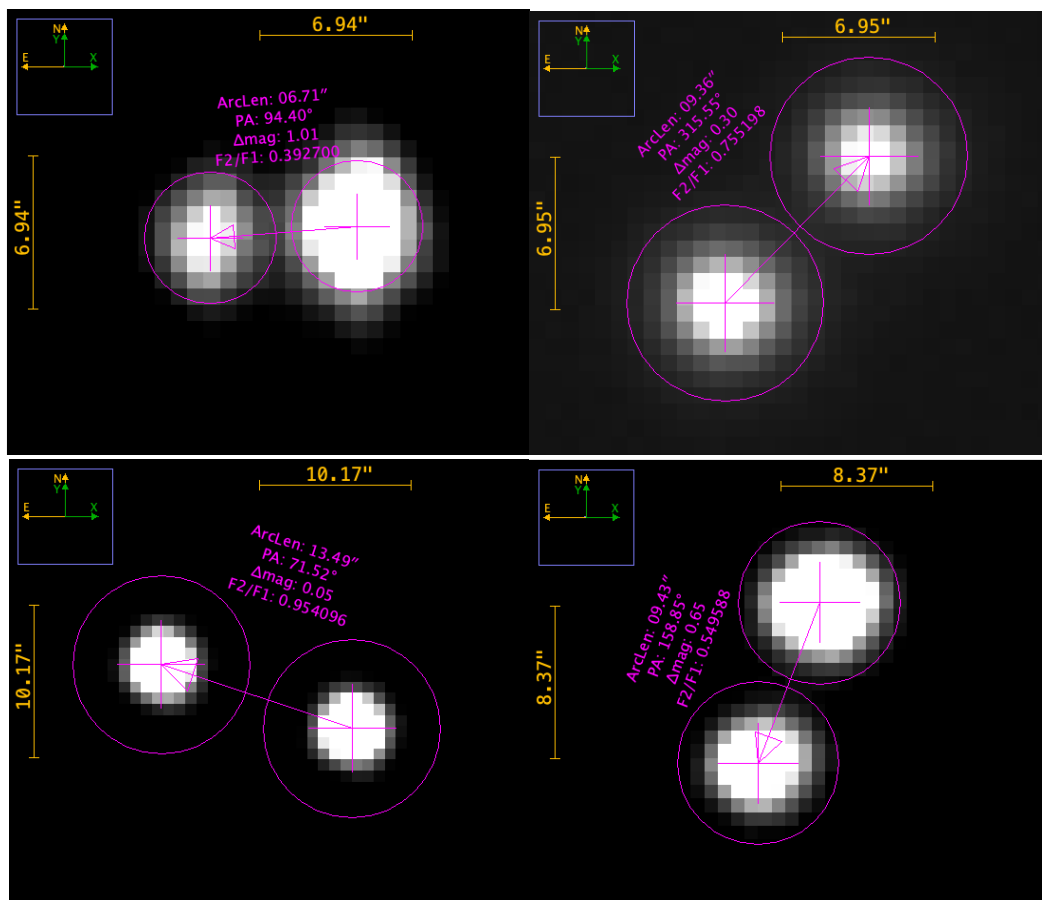


Figure 3: Sample measurements of each system using the AstroImageJ software. The separation is displayed as ‘ArcLen’ and the positional angle is displayed as ‘PA.’ Measurements are shown in the following order from top left to bottom right: HEI 915, GRV 719, STI 2170, RST 2531.

Table 2. Summary Measurements of Double Star Systems After Reduction.

System	Aperture	Date	Number	Average	Standard	Average	Standard
--------	----------	------	--------	---------	----------	---------	----------

	Size (px)		of Images	Position Angle (°)	Error on Position Angle	Separation (")	Error on Separation
HEI 915	4	2024.0329	10	93.9	0.203	6.71	0.010
GRV 719	6	2024.0437	10	315.4	0.032	9.33	0.026
STI 2170	8	2024.0380	10	71.6	0.013	13.48	0.004
RST 2531	6	2024.0329	10	158.8	0.050	9.45	0.009

#### 4. Plots

Plots of the historical measurements of each system are plotted below in Figs. 4 - 8. Gaia DR3 data measurements are shown in pink, and our measurements are shown in purple. The rest of the data points are colored chronologically, with blue data points being the oldest and red being the most recent. Note that one extreme outlier is not shown in the RST 2531 plot, due to being at a position angle of  $165^\circ$ , unlike most of the other historical data points which were around  $156^\circ$ . Also, for STI 2170, two plots are shown, the second of which has 3 outliers removed.

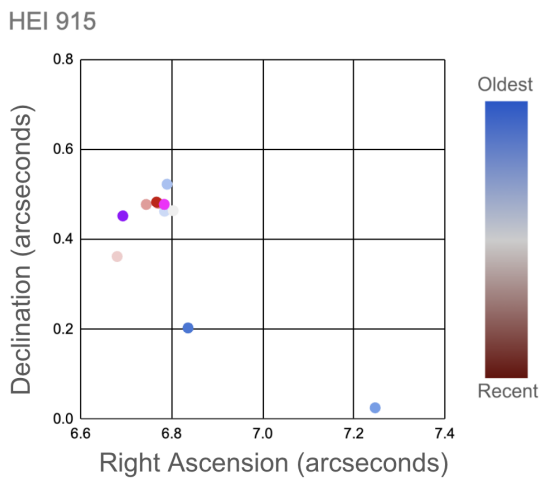


Figure 4. Measurements over time of HEI 915.

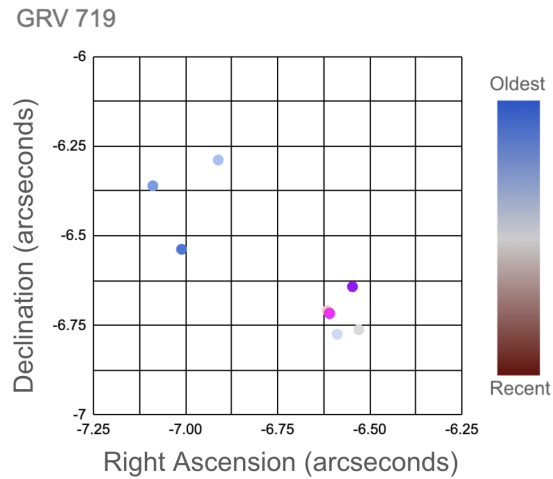


Figure 5. Measurements over time of GRV 719.

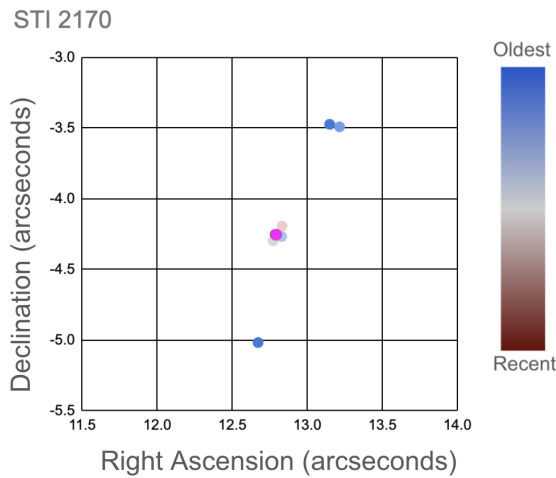


Figure 6. Measurements over time of STI 2170.

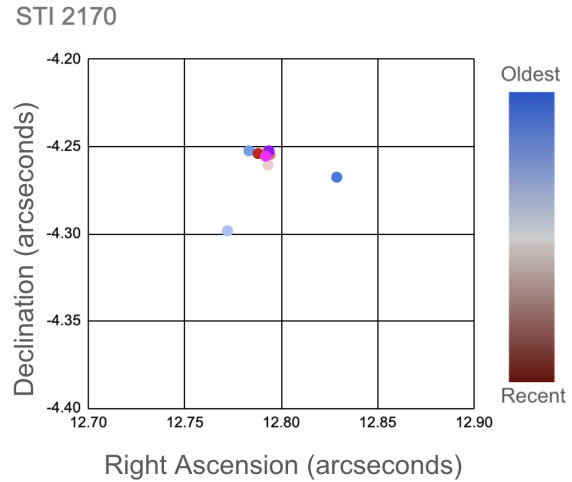


Figure 7. Measurements over time of STI 2170 with three outliers removed to see the other data points more clearly.

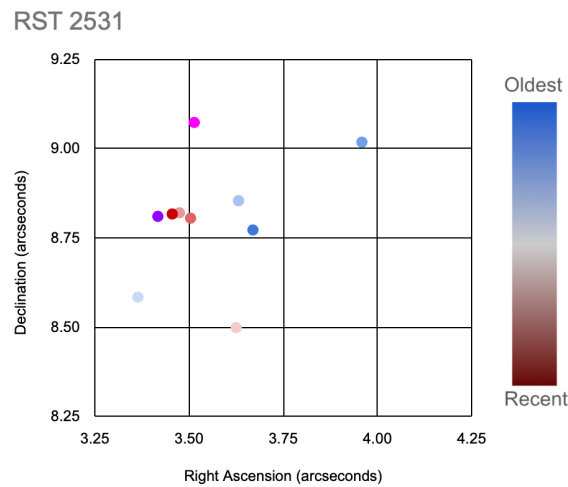


Figure 8. Measurements over time of RST 2531.

All of the plots show some roughly-linear movement of the secondary star relative to the primary, though none suggest the curvature that would be expected for a binary system. Some of the systems such as GRV 719 do not have enough measurements for curvature to be conclusive even if it were present.

### 5. Discussion

Data, shown below in Table 3, were queried from the Gaia Data Release 3 (DR3) to assess the physical relationship probability by analyzing each star's proper motion components. With these data, a relative proper motion (rPM) metric was calculated by subtracting the secondary stars' PM vector from the primary stars' PM vector and finding the magnitude of the resultant vector (Harshaw 2016). This metric compares

the relative transverse motion to the proper motion of the faster-moving one. A lower rPM value, therefore, correlates with a higher similarity of motions between the two stars in the system. As shown in Table 3, the rPM value for each system is low, indicating that the stars within each system are moving similarly and could be physically related.

Table 3. Gaia DR3 Parallaxes (Plx), Proper Motions (PM), and relative proper motion (rPM).

System	Plx Primary (mas)	Plx Secondary (mas)	PM RA Primary (mas/yr)	PM RA Secondary (mas/yr)	PM Dec Primary (mas/yr)	PM Dec Secondary (mas/yr)	rPM
HEI 915	3.45885 ± 0.02864	3.56317 ± 0.01777	1.56350 ± 0.03639	-0.52490 ± 0.02269	-19.19521 ± 0.02439	-19.44186 ± 0.01510	0.108
GRV 719	2.65366 ± 0.02152	2.63029 ± 0.01738	21.43298 ± 0.01793	21.72652 ± 0.01541	-9.23882 ± 0.01610	-9.32412 ± 0.01541	0.013
STI 2170	2.09331 ± 0.02591	2.01821 ± 0.02742	-4.16140 ± 0.01967	-5.55450 ± 0.02060	-14.40618 ± 0.01865	-13.89846 ± 0.01881	0.099
RST 2531	4.75901 ± 0.01490	5.32480 ± 0.24222	-24.27940 ± 0.01448	-26.76894 ± 0.30093	2.92426 ± 0.01549	2.24515 ± 0.26812	0.096

Additionally, the escape velocity for each system is calculated using the formula of Eq. (2), whose derivation is based on the fact that total mechanical energy of the system has to be zero for the stars to be orbiting each other (Bonifacio et al., 2020). In Eq. (2), since both stars are orbiting a common center of mass,  $M$  is the combined mass of the system (the sum of the component masses in Table 1 converted to units of kg),  $v$  refers to the system escape velocity,  $G$  is the gravitational constant, and  $r$  is the physical distance between the stars in meters.

$$v_{escape} = \sqrt{\frac{2GM}{r}} \quad (2)$$

The 3-dimensional separation  $r$  between the stars has 2 components: transverse and radial. The transverse angular separation is used to calculate a transverse physical separation in parsecs using the unit conversions shown in Eq. (3).

$$Sep_{pc} = \frac{Sep_{arcseconds} \cdot \frac{1^\circ}{3600''} \cdot \frac{2\pi rad}{360^\circ}}{parallax''} \quad (3)$$

To find the 3-dimensional separation  $r$ , the transverse separation, computed via Equation 3 is combined with the stars' radial separation (equal to the difference of their inverted parallaxes) via the Pythagorean Theorem. For systems GRV 719 and RST 2531, where the stars' radial distances are within uncertainty of each other, the transverse separation of the systems is used as the distance between the stars without the radial component, since the overlapping uncertainties could mean that the stars are the same distance from the Earth.

The relative motion was found by using the Pythagorean theorem on the relative transverse motion and relative radial motion of the stars in the system. The relative radial motion was computed by subtracting the radial velocities of the two stars, multiplying it by 1000, and taking the absolute value. The relative transverse motion was found by first getting the relative PM vector from the difference in the two stars' proper motion in RA and Dec respectively using the Pythagorean theorem, and then dividing this by the parallax of the primary, and converting to m/s from mas/yr by the conversion factor of 4740 mas/yr to m/s.

Within each system, the stars' relative motion to each other is compared to the calculated escape velocity as a way of estimating whether the stars are likely to be gravitationally bound. If the escape velocity is substantially lower than the stars' relative motion, this is unlikely, and vice versa. These calculations will be shown for one of the systems, GRV 719, for clarity.

For GRV 719, the mass estimates from Gaia were 1.50 and 1.06 solar masses for the primary and secondary star respectively, meaning the combined mass was taken as 2.56 solar masses, and was then converted to kilograms. The transverse separation, calculated with Eq. (3), was used directly for this system because the parallaxes of the two stars overlap in uncertainty, as explained above, and equals about 0.02 parsecs. This was converted to meters using the conversion factor of  $3.086E+16$  meters per parsec. Substituting these values into Eq. (2) gives us an escape velocity of 1131 m/s.

With the same system, the relative motion was found through the process outlined above, with the final value being approximately 1199 meters per second.

The calculated escape velocities for the systems are shown in Table 4, and were calculated using Eq. (2), with the mass coming from the Gaia data in Table 1. As shown in Table 4, for three of the systems—HEI 915, STI 2170, and RST 2531—the system escape velocity is significantly lower than the stars' relative motion, so these systems are unlikely to be binary. For GRV 719, however, the estimated escape velocity is close to the system's relative motion. Therefore, within the uncertainty of the calculation, the stars of GRV 719 might be gravitationally bound to each other.

Table 4. Calculated escape velocities and relative motions

System	Calculated Escape Velocity (m/s)	Relative Motion (m/s)
HEI 915	49	2900
GRV 719	1131	1199
STI 2170	32	3457
RST 2531	1570	2019

## 6. Conclusion

A new measurement of PA and Sep for each system was found from our measurements. From the Gaia DR3 (parallax and proper motion), all of the systems are physically related. The calculated rPM constant is low, which supports this. The estimated escape velocities of each system are lower than the stars' relative



velocities, which suggests that they are not binary, though the fact that the escape and relative velocities of GRV 719's components were within 70 m/s of each other makes this system less conclusive. Corroborating this, the systems' historical data plots show vaguely linear trends over time in the position of the secondary star relative to the primary. Continued measurements of these systems would help confirm these trends and to refine the calculations.

## 7. Acknowledgements

This research was made possible by the Washington Double Star catalog maintained by the U.S. Naval Observatory, the Stelle Doppie catalog maintained by Gianluca Sordiglioni, Astrometry.net, and AstroImageJ software which was written by Karen Collins and John Kielkopf.

This work has made use of data from the European Space Agency (ESA) mission Gaia (<https://www.cosmos.esa.int/gaia>), processed by the Gaia Data Processing and Analysis Consortium (DPAC, <https://www.cosmos.esa.int/web/gaia/dpac/consortium>). Funding for the DPAC has been provided by national institutions, in particular the institutions participating in the Gaia Multilateral Agreement.

This work makes use of observations taken by the Planewave Delta Rho 350 + QHY600 CMOS camera systems of Las Cumbres Observatory Global Telescope Network located in Tenerife, Spain; Texas, USA; and New South Wales, Australia.

The Las Cumbres Observatory's education network telescopes were upgraded through generous support from the Gordon and Betty Moore Foundation.

This research has made use of the SIMBAD database, operated at CDS, Strasbourg, France (Wenger et al. 2000).

This publication makes use of data products from the Two Micron All Sky Survey, which is a joint project of the University of Massachusetts and the Infrared Processing and Analysis Center/California Institute of Technology, funded by the National Aeronautics and Space Administration and the National Science Foundation.

Thank you to our reviewer from JDSO for the insightful and helpful comments.

## 8. References

- Bonifacio, B., C. Marchetti, R. Caputo, and K. Tock. (2020). Measurements of Neglected Double Stars. *Journal of Double Star Observations*, 16(5), 411–423.  
[http://www.jdso.org/volume16/number5/Bonifacio\\_411\\_423.pdf](http://www.jdso.org/volume16/number5/Bonifacio_411_423.pdf)
- Bronnikova, N. M. (1975). Stars suspected of variability in the Taurus region. *Peremennye Zvezdy Prilozhenie*, 2(10), 225–236.
- Brown, T. M. et al. (2013). Las Cumbres Observatory Global Telescope Network. *Publications of the Astronomical Society of the Pacific*, 125(931), 1031–1055.  
<https://iopscience.iop.org/article/10.1086/673168/meta>
- El-Badry, K., Rix, H., Heintz, T. (2021). A million binaries from Gaia eDR3: sample selection and validation of Gaia parallax uncertainties. *Monthly Notices of the Royal Astronomical Society*, 506(2), 2269–2295.
- Gaia Collaboration, T. Prusti, J.H.J. de Bruijne, et al. (2016b). The Gaia mission. *A&A* 595, A1.  
[https://www.aanda.org/articles/aa/full\\_html/2016/11/aa29272-16/aa29272-16.html](https://www.aanda.org/articles/aa/full_html/2016/11/aa29272-16/aa29272-16.html)
- Gaia Collaboration, A. Vallenari, A. G. A. Brown, et al. (2023j) Gaia Data Release 3. Summary of the content and survey properties. *A&A* 674, pp. A1. <https://arxiv.org/abs/2208.00211>
- Gaia Collaboration, C. Babusiaux, C. Fabricius, S. Khanna, et al. (2023) Gaia Data Release 3. Catalogue validation. *A&A* 674, pp. A32. <https://arxiv.org/abs/2206.05989>
- Harshaw, Richard (2016). CCD Measurements of 141 Proper Motion Stars: The Autumn 2015 Observing Program at the Brilliant Sky Observatory, Part 3. *Journal of Double Star Observations*, 12(4), 394–399. [http://www.jdso.org/volume12/number4/Harshaw\\_394\\_399.pdf](http://www.jdso.org/volume12/number4/Harshaw_394_399.pdf)
- L. Ruiz-Dern, C. Babusiaux, et al. (2018). Empirical photometric calibration of the Gaia red clump: Colours, effective temperature, and absolute magnitude. *A&A* 609, A116.  
[https://www.aanda.org/articles/aa/full\\_html/2018/01/aa31572-17/aa31572-17.html](https://www.aanda.org/articles/aa/full_html/2018/01/aa31572-17/aa31572-17.html)
- Skrutskie, M. F. et al. (2006). The Two Micron All Sky Survey. *The Astronomical Journal*. 131(2), 1163–1183.
- Tonry, J. L, et al. (2012). The PanStarrs1 Photometric System. *The Astrophysical Journal*.  
<https://iopscience.iop.org/article/10.1088/0004-637X/750/2/99/pdf>
- Zacharias, N. et al. (2015). The First U.S. Naval Observatory Robotic Astrometric Telescope Catalog. *The Astronomical Journal*, 150(4), 101.  
<https://ui.adsabs.harvard.edu/abs/2015AJ....150..101Z/abstract>